scientific reports

Check for updates

OPEN

Genome-wide profiling of circulating microRNAs in adolescent idiopathic scoliosis and their relation to spinal deformity severity, and disease pathophysiology

Nasrin Khatami[1,2], Iurie Caraus[1,2], Mahamuda Rahaman[1], Evguenia Nepotchatykh[1,3], Mohamed Elbakry[1,4], Wesam Elremaly[1], Anita Franco[1], Marie Beauséjour[5,6,7], Anne-Marie Laberge[8], Stefan Parent[5,6,9,10], Hubert Labelle[5,6,9,10], Carl-Éric Aubin[5,10,11], Jean Lachaine[12] & Alain Moreau[1,2,3,10,13]✉

Adolescent Idiopathic Scoliosis (AIS) is the most common orthopedic condition requiring surgery, affecting 4% of adolescents. There is currently no proven method or prognostic test to identify symptomatic patients at risk of developing severe scoliosis who could benefit from growth-guided devices or minimally invasive non-fusion instrumentation surgeries. These innovative treatments must be performed at an early disease stage in younger patients to benefit from their growth potential. In this prospective cross-sectional study, we investigated the clinical utility of circulating microRNAs (miRNAs), an important class of small non-coding RNA, as biomarkers to predict the risk of developing severe scoliosis in AIS. Blood samples and clinical data were collected from 116 AIS patients who were followed until skeletal maturity and stratified according to their clinical outcome. Genome-wide expression profiling of miRNAs was performed with plasma obtained at the time of diagnosis of AIS (mean age of 13.3 ± 1.7 years with a mean Cobb angle of 24.4° ± 12.4°). This approach led to the identification of 15 circulating miRNAs that are upregulated in AIS patients who developed a severe scoliosis (Cobb angle ≥ 45°) at skeletal maturity compared to moderate and mild scoliosis groups (Cobb angle between 25°-44° and < 25° respectively). After optimization and the application of Random Forest Models a panel of six miRNAs (miR-1-3p, miR-19a-3p, miR-19b-3p, miR-133b, miR-143-3p, and miR-148b-3p) out of 15 led us to develop an algorithm predicting the risk of developing a severe scoliosis with great accuracy (100%), sensitivity (100%) and specificity (100%). Having a scoliosis predictive bioassay and decision-making tools to predict curve progression in order to find the best treatment plan will undoubtedly transform the orthopedic care system in the field of pediatric scoliosis by integrating innovative precision medicine approaches. In addition, investigation of genes targeted by these miRNAs could fill our gaps in our understanding of AIS pathogenesis and reveal new actionable targets.

Keywords Adolescent idiopathic scoliosis, Circulating microRNAs, Spinal deformity severity, Disease pathophysiology, Diagnostic and prognostic biomarkers, Machine learning

[1]Viscogliosi Laboratory in Molecular Genetics of Musculoskeletal Diseases, Azrieli Research Center, CHU Sainte-Justine, room 2.17.027, 3175 Cote-Ste-Catherine Road, Montreal, QC H3T 1C5, Canada. [2]Department of Biochemistry and Molecular Medicine, Faculty of Medicine, Université de Montréal, Montreal, QC, Canada. [3]Molecular Biology PhD Program, Faculty of Graduate and Postdoctoral Studies, Université de Montréal, Montreal, QC, Canada. [4]Biochemistry Division, Chemistry Department, Faculty of Science, Tanta University, Tanta, Egypt. [5]Azrieli Research Center, CHU Sainte-Justine, Montreal, QC, Canada. [6]Department of Surgery, Faculty of Medicine, Université de Montréal, Montreal, QC, Canada. [7]Department of Community Health Sciences, Faculty of Medicine and Health Sciences, Université de Sherbrooke, Longueuil, QC, Canada. [8]Medical Genetics, Department

	AIS (progressor/non-progressor)		Healthy control
N	34P	35NP (7MOP/ 28NP)	14 HC
Age (years)	13.9 ± 1.6	14.4 ± 2.4	11.1 ± 0.2
Sex	21F/13M	20F/15M	9F/5M
Cobb angle	35.1° ± 15.7°	17.2° ± 6.6°	–

Table 1. Clinical and demographic characteristics of participants-discovery cohort. Data are expressed as a mean ± standard deviation. *P* progressors, *NP* non-progressors, *MOP* moderate progressors, *HC* healthy controls, *F* females, *M* males.

	AIS (progressor/non-progressor)		Healthy control
N	6P	6NP	6 HC
Age (years)	11.5 ± 0.7	12.3 ± 0.7	10.5 ± 0.6
Sex	6 F	6 F	5 F/1 M
Cobb angle	30.5° ± 6.9°	17.8° ± 5.6°	-

Table 2. Clinical and demographic characteristics of participants-validation cohort 1. Data are expressed as a mean ± standard deviation. *P* progressors, *NP* non-progressors, *HC* healthy controls, *F* females and *M* males.

of Pediatrics, CHU Sainte-Justine and Université de Montréal, Montreal, QC, Canada. [9]Orthopedic Division, CHU Sainte-Justine, Montreal, QC, Canada. [10]Institut TransMedTech Montreal, CHU Sainte-Justine, Montreal, QC, Canada. [11]Polytechnique Montréal, Montreal, QC, Canada. [12]Faculty of Pharmacy, Université de Montréal, Montreal, QC, Canada. [13]Department of Stomatology, Faculty of Dentistry, Université de Montréal, Montreal, QC, Canada. ✉email: alain.moreau.hsj@ssss.gouv.qc.ca

Adolescent Idiopathic Scoliosis (AIS) is one of the most common childhood deformities worldwide. It is characterized by a tridimensional spinal deformity with unknown causes, representing both an immediate medical challenge and a chronic condition affecting individuals throughout their lives. It is the most common orthopedic condition requiring surgery in adolescents and affects 2–4% of this population[1]. Unfortunately, no proven method or test is available to identify, at an early stage, symptomatic adolescents at risk of developing a severe scoliosis. Consequently, the application of current treatments, such as bracing or surgical correction, are delayed until a significant deformity is detected or until a significant progression is clearly demonstrated, resulting in costly and less than optimal treatments.

Given the clinical heterogeneity of the disease, biological sex differences (higher prevalence in girls) and potential crosstalk with undefined environmental factors, a search for epigenetic factors has been undertaken. Among key epigenetic mechanisms, microRNAs (miRNAs) have emerged as an essential class of small non-coding RNAs that suppress the translation and/or stability of specific mRNA targets in different human diseases by binding to 3'UTR sites of targeted mRNAs. Indeed, previous studies revealed differentially expressed miRNAs in plasma, serum and bone derived cells associated with AIS[2–15]. However, the exact role of these miRNAs in scoliosis is not yet fully understood, but they are likely involved in several different pathways that contribute to the development and progression of the disease.

In this study, we aimed to identify circulating miRNAs, which in combination with machine-learning approaches that could predict, the development of severe scoliosis (Cobb angle ≥ 45°) at the earliest possible stage. We also aimed to discriminate symptomatic patients with a risk of moderate disease progression (Cobb angle between 25°–44°) from those with a minimal progression potential (Cobb angle < 25°) compared to matched healthy controls.

Results

Study populations

This cross-sectional study is part of a larger longitudinal prospective study conducted in three pediatric spine centers. The participants were recruited from June 2002 to August 2013, and data collection was completed in June 2016. Healthy controls (HC) without a family antecedent of scoliosis were recruited during the same period from primary and high schools from the Greater Montreal's area. The clinical and demographic characteristics of our discovery cohort are reported in Table 1. Stratification by scoliosis severity was determined only in the participants who have completed their longitudinal follow-up and reached their skeletal maturity. This discovery cohort consisted of 34 AIS patients (21 F/13 M) classified as spinal deformity progressors (P), 35 AIS patients (20 F/15 M) classified as non-progressors (NP), and 14 matched healthy controls (9 F/5 M). Table 2 shows the characteristics of our initial validation cohort used to assess the capacity of our qPCR probes to amplify our candidate miRNAs. This second cohort was composed of six female AIS patients classified as spinal deformity progressors (P), six female AIS patients classified as non-progressors (NP), and six matched healthy controls (5 F/ 1 M). Table 3 shows the characteristics of our replication cohort, which was composed of 15 AIS patients

	AIS (progressor/non-progressor)		Healthy control
N	15P	20NP (9MOP /11NP)	10 HC
Age (years)	13.1 ± 1.6	13.6 ± 1.6	12.0 ± 1.8
Sex	11 F/4 M	11 F/9 M	4 F/6 M
Cobb angle	26.4° ± 3.9°	18.2° ± 6.2°	–

Table 3. Clinical and demographic characteristics of participants - validation cohort 2. Data are expressed as a mean ± standard deviation. *P* progressors, *NP* non-progressors, *MOP* moderate progressors, *HC* healthy controls, *F* females and *M* males.

(11 F/4 M) classified as spinal deformity progressors (P), 20 AIS patients (11 F/9 M) classified as non-progressors, and 10 matched healthy controls (4 F/6 M).

Subclassification of AIS patients with scoliosis progression less than 45°

Initially, we grouped all patients diagnosed with AIS and exhibiting a spinal deformity less than 45° (considering only the main curve) at skeletal maturity as the non-progressor (NP) group. However, we observed that these patients could be categorized into two distinct groups. Indeed, some patients displayed a Cobb angle progression of more than 15° overtime, leading us to classify them as moderate progressors (MOP). Conversely, patients exhibiting a progression of less than 15° were classified as non-progressors (NP). We applied this refined stratification during our replication cohort, resulting in the classification of 9 patients in the MOP group (6 F/3 M) and 11 (5 F/6 M) in the NP group.

Identification of circulating miRNAs associated with AIS

We conducted a comprehensive genome-wide expression profiling of circulating miRNAs using plasma samples from our discovery cohort. We employed the Agilent expression array-Human miRNA 8 × 60 K chips to identify candidate circulating miRNAs differentially expressed in AIS patients compared to HC group. Our initial screening revealed 90 candidate miRNAs exhibiting the most significant fold change with a P value < 0.05 (Supplementary Table S1).

Validation and replication assays of identified circulating miRNAs

Selected candidate miRNAs were validated initially by RT-qPCR using a distinct small cohort of AIS patients ($n = 12$) and HC ($n = 6$) (Table 2). The fold difference in miRNA expression between each patient and the mean of HC group was calculated as $2^{(-\Delta\Delta CT)}$. Of note, we were able to amplify only 70 miRNAs out of 90 initially discovered using the Agilent microarray (Supplementary Table S2). Subsequently, these 70 miRNAs were validated in a larger cohort comprising 35 AIS patients and 10 matched HC (Table 3). Among the 70 candidate miRNAs, 15 miRNAs (let-7f-5p, miR-1-3p, miR-18a-3p, miR-19a-3p, miR-19b-3p, miR-103a-3p, miR-107, miR-133b, miR-143-3p, miR-148a-3p, miR-148b-3p, miR-152-3p, miR-214-3p, miR-551b-3p, and miR-576-5p) were significantly upregulated in AIS P group developing a severe scoliosis (Cobb angle ≥ 45°) compared to MOP + NP group developing mild-to-moderate scoliosis (Cobb angle 10°–44°) (Figs. 1 and 2).

Sex-specific differences in circulating miRNA expression

Given the higher prevalence of AIS in females compared to males, we conducted a more in-depth investigation into how biological sex impacts the expression profile of our panel of miRNAs. Intriguingly, we observed distinct expression patterns depending on the severity of the disease in each sex. In females, one of the 65 miRNAs, miR-18a-3p, was significantly upregulated in the female severe group (FP) compared to the females classified in the non-severe group (FMOP + FNP), as shown in Supplementary Figure S1. On the other hand, in males, two miRNAs miR-103a-3p, and miR-107 were significantly downregulated in the male non-progressor group (MNP) compared to healthy controls (Supplementary Figure S2). Additionally, miR-551b-3p and miR-4665-5p displayed significant upregulation in the male moderate progressor group (MMOP) compared to the male non-progressor group (MNP) (Supplementary Figure S3). It is noteworthy to mention that miR-4665-5p, although not initially included in our top 15 miRNAs, emerged as a key miRNA associated with moderate spinal deformity progression in male patients with AIS.

AIS-associated circulating miRNAs and prediction of scoliosis severity

We evaluated the clinical utility of our panel of 15 circulating miRNAs to predict the development of a severe scoliosis using the Random Forest Model (RFM). We first applied RFM to a randomly selected training dataset representing 80% of all our AIS cases. We then challenged the performance of our models using the remaining 20% of our AIS cases as testing dataset. We generated receiver operating characteristic curves (ROC curves) and obtained the following results. When classifying patients with severe scoliosis (P) versus patients with mild scoliosis (NP), a panel of six miRNAs (miR-1-3p, miR-19a-3p, miR-19b-3p, miR-133b, miR-143-3p, miR-148b-3p) showed an accuracy, specificity, and sensitivity of 100%, with a ROC curve AUC = 1.0 in predicting the risk of developing a severe scoliosis in symptomatic patients from both sexes (Supplementary Figure S4a). The inclusion of all 15 miRNAs in our algorithm slightly reduced the accuracy (90%) and specificity (88%) of the test, without affecting its sensitivity (100%) (Supplementary Figure S4b). Interestingly, in the context of sex specific miRNAs, two additional panels of miRNAs can predict female curve progression with the accuracy, specificity and the sensitivity of 100% and a ROC AUC = 1.0. The first panel includes seven miRNAs (miR-1-3p, miR-18a-3p, miR-

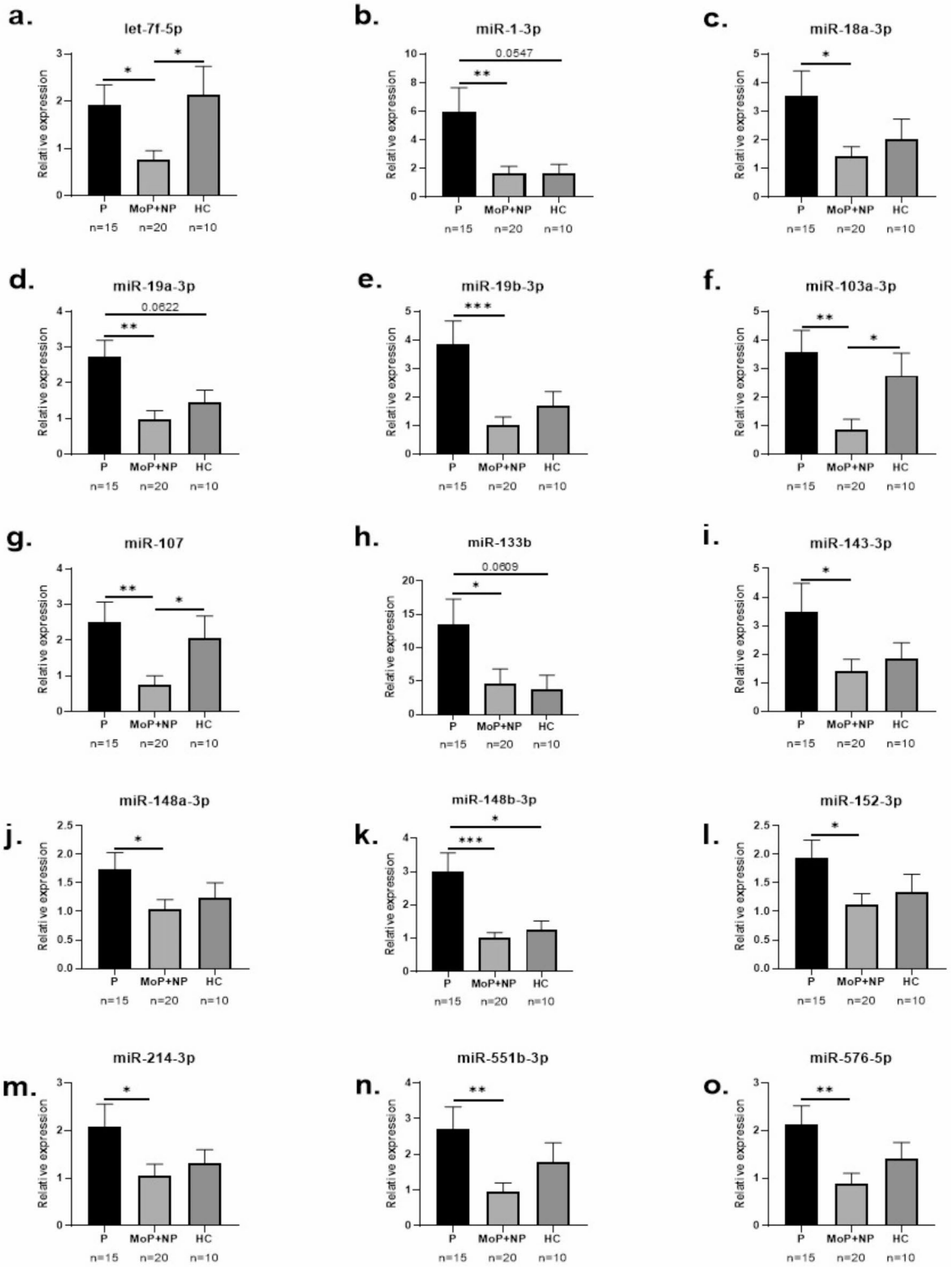

Fig. 1. Top 15 circulating miRNAs upregulated in severe AIS cases. Panel a to o represent the expression analysis of let-7f-5p, miR-1-3p, miR-18a-3p, miR-19a-3p, miR-19b-3p, miR-103a-3p, miR-107, miR-133b, miR-143-3p, miR-148a-3p, miR-148b-3p, miR-152-3p, miR-214-3p, miR-551b-3p, and miR-576-5p respectively. A comparison of relative expression level for each miRNA was performed between the severe or progressor group (P) vs. the non-severe group, including moderate progressor + non-progressor (MoP + NP). GraphPad Prism 9 was used to generate graphs and statistical analysis. Statistical significance between each group was determined using the T-test for two groups and ANOVA for more than two groups (*p-value < 0.05, **p-value < 0.01, ***p-value < 0.001).

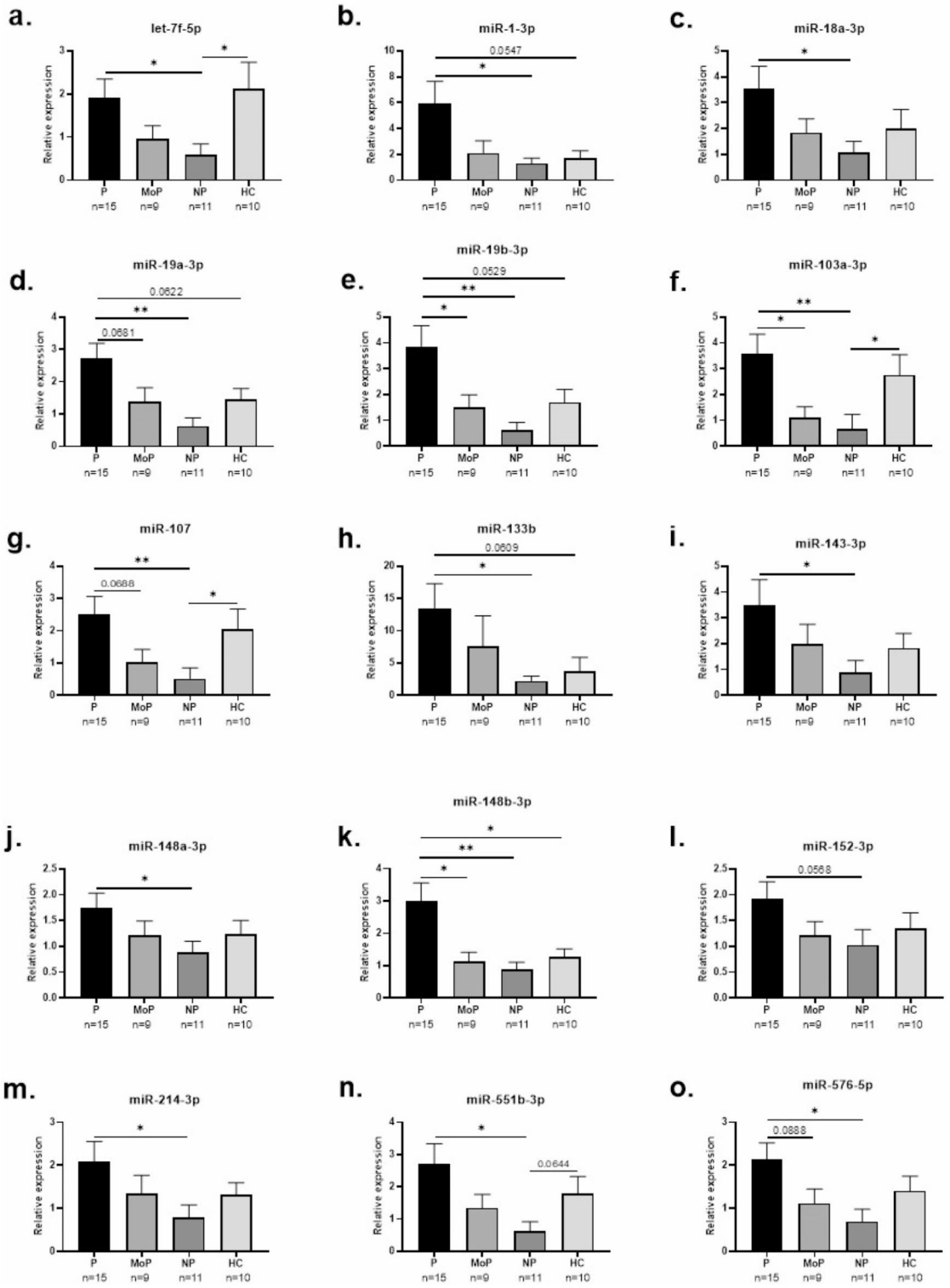

Fig. 2. Top 15 miRNAs upregulated in AIS progressor group (P) compared to moderate (MOP) and non-progressor (NP) groups. Panel a to o represent the expression analysis of let-7f-5p, miR-1-3p, miR-18a-3p, miR-19a-3p, miR-19b-3p, miR-103a-3p, miR-107, miR-133b, miR-143-3p, miR-148a-3p, miR-148b-3p, miR-152-3p, miR-214-3p, miR-551b-3p, and miR-576-5p respectively. These 15 miRNAs were upregulated in severe group (P) non-progressor (NP) groups. Three (miR-19b-3p, miR-103a-3p, miR-148b-3p) miRNAs were significantly upregulated between severe group (P) and moderate progressor group (MOP). GraphPad Prism 9 was used to generate graphs and statistical analysis. Statistical analysis. Statistical significance between each group was determined using the T-test for two groups and ANOVA for more than two groups (*p-value < 0.05, **p-value < 0.01).

19a-3p, miR-19b-3p, miR-133b, miR-143-3p, miR-148b-3p) (Supplementary Figure S4c). The second panel includes four miRNAs (let-7f-5p, miR-18a-3p, miR-103a-3p, miR-551b-3p) (Supplementary Figure S4d). Also, we identified two miRNAs (miR-551b-3p and miR-4665-5p) predicting moderate spinal deformity progression in males with a similar accuracy, specificity and the sensitivity of 100% and a ROC AUC = 1.0 (Supplementary Figure S4e).

Gene pathways and network analysis

We conducted a systematic gene pathway and network analysis to better understand our selected miRNAs' mechanistic contribution in AIS pathogenesis. Our gene pathway analyses using the Ingenuity Pathway Analysis (IPA) software revealed that majority of the 15 miRNAs were primarily involved in muscle dystrophy, skeletal muscular disorders, muscle overgrowth, cardiac muscle disorders, progressive dystrophy, and other muscles related diseases (Supplementary Figure S5). Indeed, two of our miRNAs (miR-1-3p and miR-133b) have been previously identified as myomiRs[16]. We then applied a hybrid approach combining IPA and manual curations. We first searched the literature and manually identified genes and molecules reported to be associated with AIS or scoliosis. We then built connections with each of the 15 miRNAs, and these genes and functions based on the IPA experimentally observed Ingenuity Knowledge Base. This comprehensive analysis allowed us to construct more complete networks that connected each miRNA to its targets (e.g., AIS-related genes) that could play critical roles in the pathogenesis of AIS. Using the IPA and manual curation hybrid approach, we further constructed a larger and more complete network connecting these 15 miRNAs and their key genes and disease targets. Similar approach by integrating previous scoliosis severity associated miRNAs from the literature showed that these miRNAs (miR-96-5p, miR-145-5p, miR-151a-3p) share common targets with the targets of our 15 candidate miRNAs (Fig. 3).

Discussion

The underlying molecular mechanisms that cause AIS onset and those associated with spinal deformity progression remain poorly understood. On the other hand, the epigenetic landscape of AIS is a largely unexplored field of research that may explain the variability of scoliosis progression and the fact that 85% of AIS cases occur in individuals without familial antecedents of scoliosis[1]. In this study, we identified 15 circulating miRNAs (let-7f-5p, miR-1-3p, miR-18a-3p, miR-19a-3p, miR-19b-3p, miR-103a-3p, miR-107, miR-133b, miR-143-3p, miR-148a-3p, miR148b-3p, miR-152-3p, miR-214-3p, miR-551b-3p, and miR-576-5p) associated with AIS and scoliosis severity. Using RFM, we found that six of these miRNAs (miR-1-3p, miR-19a-3p, miR-19b-3p, miR-133b, miR-143-3p, and miR-148b-3p) can accurately predict the development of severe scoliosis in symptomatic AIS patients of both sexes at their first medical visit.

Among our 15 candidate miRNAs, upregulation of miR-18a-3p was previously reported to be associated with AIS[17]. Also, downregulation of miR-107 was found associated with AIS severity[11]. Thirteen remaining circulating miRNAs are novel and were not reported by other research group before and can be attributed to our distinctive study design, and robust sample size. The biological relevance of our predictive panel of six circulating miRNAs in AIS pathogenesis is further supported by the fact that several genes targeted by these miRNAs, encode for proteins that were previously reported to be associated with AIS. Also, the AIS severity associated miRNAs from the previous literature (miR-96-5p, miR-145-5p, miR-151a-3p) are sharing common targets with our panel of 15 miRNAs, which further strengthens their role in spinal deformity progression. For instance, let-7f-5p is predicted to target dual specificity phosphatase 6 (DUSP6) gene. DUSP6 gene expression was reported as downregulated in a microarray analysis on the bone marrow stromal cells (MSC) and at the mRNA levels in ligament tissues of AIS patients compared to healthy control. A protein–protein interaction (PPI) network analysis showed that DUSP6 is associated with MAPK signaling pathway[12]. *DUPS6* is also targeted by miR-145-5p, which is a scoliosis severity associated miRNA, upregulated in AIS osteoblasts[6].

Among known or predicted targets for miR-1-3p, we identified *FN1*, which encodes fibronectin 1, and while its role in AIS pathogenesis remains to be investigated, mutations in *FN1* gene have been recently identified to cause of a rare form of skeletal disorder called spondylometaphyseal dysplasia, which is associated with scoliosis[18]. Similarly, miR-1-3p also targets *NOTCH2* gene (Notch 2 receptor), which is mutated in a very rare illness called Hajdu-Cheney syndrome (HCS). This mutation is associated with a range of skeletal abnormalities, including severe osteoporosis, resulting in a significant risk of developing progressive spinal deformities such as scoliosis[19]. On the other hand, miR-151a-3p (upregulated in serum and osteoblasts of severe AIS cases)[11] and miR-96-5p (upregulated in female AIS osteoblasts)[14] were previously introduced as scoliosis severity associated miRNAs, and both target *FN1*. Collectively, our results and previous studies indicates the importance of FN1 as a possible disease-modifying factor in AIS and further studies are required to unveil the exact pathomechanism of FN1 in AIS severity. Among other targets of miR-1-3p, we found UTSR2, which codes for the urotensin ii receptor, and a recent study by Dai et al., showed the presence of novel mutations in the UTSR2 gene associated with AIS in Chinese population[20]. While the role of urotensin ii (UTS2) signaling in AIS pathomechanism is poorly understood, dysregulated UTS2 signals induced by impaired cerebrospinal fluid flow have been associated with the development of idiopathic scoliosis in zebrafish studies[21]. Interestingly, a second miRNA in our AIS prognostic panel, miR-18a-3p, is targeting UTS2, which further strengthens the proposed role of UTS2/UTSR2 signaling in AIS pathogenesis. Therefore, the elevation of miR-1-3p and miR-18a-3p expression is most likely contributing to a UTS2 signaling dysfunction (at least in Caucasians) resulting in spinal deformity progression. Interestingly, our analyses also unveiled that miR-18a-3p expression was upregulated in females progressors developing a severe scoliosis, suggesting that this miRNA could contribute to sex-related difference observed in AIS pathogenesis. Among other targeted genes common to miR-1-3p and miR-18a-3p, we found CRTAP gene, which codes for the cartilage-associated protein. CRTAP mutations usually cause severe osteogenesis imperfecta (OI) often resulting to a severe scoliosis phenotype[22].

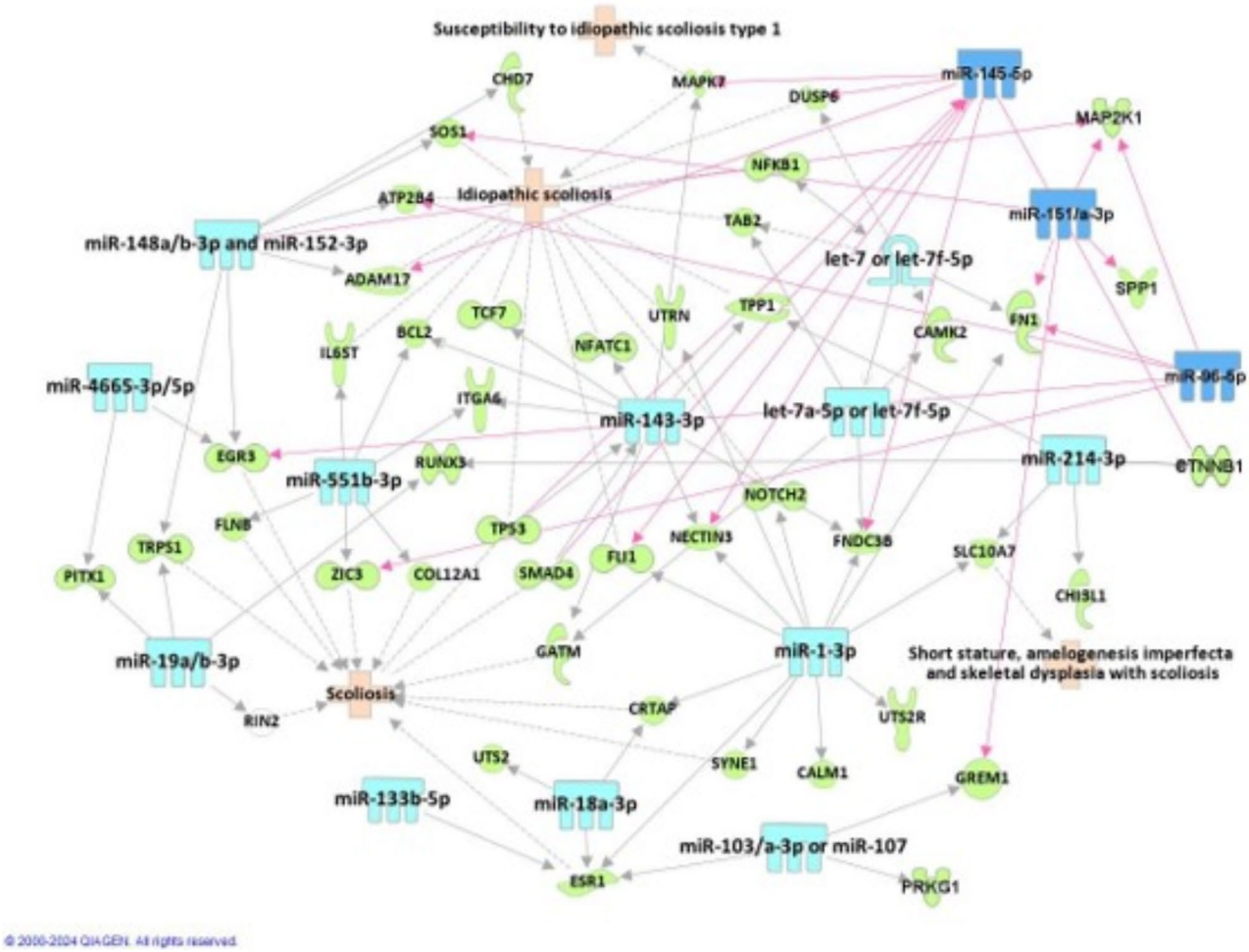

Fig. 3. Predicted pathway and network of top 15 miRNAs associated with AIS and scoliosis severity. The potential targets of these 15 miRNAs and previously discovered AIS severity associated miRNAs, including genes, molecules and their connection to idiopathic scoliosis or scoliosis phenotype, are shown in one integrated network. Our 15 candidate miRNAs are represented in light blue; AIS severity associated miRNAs are in dark blue, their interaction with targets indicated with pink lines; the genes predicted to interact are in green; the diseases associated with miRNAs or genes are in light pink. The Ingenuity Pathway Analysis (IPA) software (QIAGEN Inc. software version 51963813) and manual curations were applied to construct the network.

Elevation of circulating miR-19a-3p and miR-4665-3p levels (the later one only in males) and their association with scoliosis severity in AIS is also supported by the work of Fendri et al., who showed a severe downregulation of the transcription factor PITX1 (a known target of miR-19a-3p and miR-4665-3p) in osteoblasts derived from intraoperative bone biopsies obtained of severe AIS cases from our cohort[23]. Moreover, Shi et al., reported a decreased *PITX1* gene expression in peripheral blood mononuclear cells (PBMCs) obtained from AIS patients through a different epigenetic mechanism involving DNA hypermethylation[24]. Their pilot study showed that increased DNA methylation levels correlated with low *PITX1* expression and were associated with curve progression in Chinese AIS patients[24]. Given that DNA methylation alterations are tissue or cell specific[25], and they may vary according to race/ethnicity and ancestry[26], it remains unclear, which epigenetic mechanisms (miRNAs vs. DNA methylation) is predominantly involved in spinal deformity progression in the context of AIS. However, both mechanisms are not mutually exclusive and may contribute to AIS pathogenesis by targeting *PITX1* gene.

Among other supporting interactions, miR-143-3p is predicted to target *MAPK7* gene, encoding for the mitogen-activated protein kinase 7, which is a common target with miR-145-5p. Rare coding variants in this gene were previously reported to predispose to AIS in Chinese population[27,28]. Remarkably, we also found that miR-148b-3p targets *ATP2B4* gene encoding for the ATPase plasma membrane Ca^{2+} transporting 4 protein (PBMC4b), which was previously reported to be decreased in osteoblasts derived from a subset of our severe AIS patients, which further supports the link between this miRNA and scoliosis severity[29]. *ATP2B4* is also targeted by miR-96-5p. Moreover, miR-148b-3p is known to target *CHD7* gene encoding for the Chromodomain Helicase DNA Binding Protein 7. *CHD7* is also mutated in AIS and was suggested to be part of a predictive loci

for AIS curve progression[30,31]. Of the remaining top 15 circulating miRNAs associated with spinal deformity progression in AIS, miR-214-3p is particularly interesting. This miRNA targets *CHI3L1* gene, which encodes for the YKL-40 glycoprotein. We previously demonstrated that plasma YKL-40 level were elevated in AIS non-progressors than in progressors, suggesting its role as a disease-modifying factor in AIS[32].

Sex differences in miRNA expression have been observed in a variety of diseases. In this study, we also investigated the impact of biological sex on the expression profile of a panel of 15 miRNAs in AIS patients. We found that there were significant differences in miRNA expression between male and female patients, and that these differences were associated with the severity of the disease. In female patients, we found that a single miRNA, miR-18a-3p, was upregulated specifically in female progressors. This finding is supported by previous studies that have shown that upregulation of miR-18a-3p is associated with a wide range of diseases related to women conditions, including breast cancer[33], endometriosis[34], and preeclampsia[35]. This suggests that estrogens may play a role in regulating the expression of this miRNA[36]. The combination of (miR-1-3p, miR-18a-3p, miR-19a-3p, miR-19b-3p, miR-133b, miR-143-3p, miR-148b-3p) or (let-7f-5p, miR-18a-3p, miR-103a-3p, miR-551b-3p) can successfully predict spinal deformity progression in symptomatic AIS females. In male patients, we found that three miRNAs, let-7f-5p, miR-103a-3p, and miR-107, were significantly downregulated in non-progressors compared to healthy controls. This suggests that the downregulation of these miRNAs may have a protective effect against AIS progression in male patients. However, we also found that the upregulation of miR-551b-3p and miR-4665-5p was associated with a moderate progression of spinal deformities in male patients and could be used as a distinctive panel to predict such risk in male patients. The discrepancies in the expression of miRNAs between male and female patients may be explained by the fact that sex hormones, such as estrogens and testosterone, play a role in regulating miRNA biogenesis and expression. Collectively, our findings underscore the importance of considering sex-specific differences in miRNA expression patterns when studying AIS progression.

Our study provides novel insights into the use of circulating miRNAs as distinctive epigenetic signatures to predict spinal deformity progression and scoliosis severity in AIS. However, it has some limitations. First, our study was conducted in a homogeneous population of Caucasians from European ancestry. This needs to be replicated in more diverse pediatric populations and larger AIS cohorts. Additionally, while many predicted or known targets of our selected miRNA panel are implicated in AIS pathogenesis and rare disorders associated with a severe scoliosis phenotype, functional assays at the cellular level or using animal models are needed to confirm these targets as well as the novel ones identified in this study.

In conclusion, our findings contribute to filling the gaps in our understanding of the molecular basis of AIS pathogenesis. Early detection of the risk of disease progression with a panel of predictive miRNAs could be a game changer in the field of orthopedics. It could broaden the range of treatment options and improve overall effectiveness and cost- effective outcomes. This study has the potential to pave the way for the development of advanced modeling techniques that can simulate orthopedic treatments and protocols prior to surgical interventions. By leveraging predictive models, healthcare professionals can better understand the outcomes of different treatment strategies. For example, refine surgical planning and optimize preoperative care, or opt for less invasive options (growth-guided devices or minimally invasive non-fusion surgeries) which can be both effective and cost-efficient. Indeed, symptomatic patients at-risk of developing a severe scoliosis could benefit, if detected at the right time, from novel posterior spinal fusion or growth-guided devices as well as recently introduced minimal-invasive non-fusion instrumentation surgeries. However, to be effective, such innovative treatments must be performed at an early disease stage in younger patients to benefit from their growth potential or the ability to achieve the best correction. The predictive miRNA panel could complement existing clinical tools to enable earlier intervention, potentially improving outcomes and reducing costs through personalized treatment strategies, ultimately improving surgical success rates and reducing recovery time.

Methods

Study design and populations

This cross-sectional study is part of a larger longitudinal prospective study conducted in three pediatric spine centers. The participants were recruited from June 2002 to August 2013, and data collection was completed in June 2016. Healthy controls (HC) without a family antecedent of scoliosis were recruited during the same period from primary and high schools from the Greater Montreal's area. The inclusion criteria concerned children aged 13.3 ± 1.7 years enrolled at their initial appointment at the scoliosis clinic with a history and physical examination consistent with AIS diagnosis. The diagnosis was confirmed by radiography with a minimum curvature in the coronal plane of 10° (mean Cobb angle value of 24.4 ± 12.4), showed by a standing postero-anterior spinal radiograph, by the Cobb method with vertebral rotation and without any known congenital or genetic disorder. All participants were skeletally immature with a Risser sign between 0 and 2, no prior treatment, and female participants were either at pre-menarche or less than one-year post-menarche. All AIS patients were followed until they reached their skeletal maturity (Risser sign of 4 or 5) or underwent surgery for a spinal deformity correction. 116 AIS patients met our eligibility criteria, which allowed their stratification according to their clinical outcome. We categorized our AIS patients into three groups. The first group developed over time a severe scoliosis (final Cobb angle ≥ 45°) requiring corrective spinal surgery and represents severe disease progressors (P). The second group was considered non-progressors exhibiting moderate curve progression (MOP) exhibiting a scoliosis with a final Cobb angle varying between 25° to 44° at skeletal maturity and avoided surgery. The third group, termed non-progressors (NP), represents individuals who did not exhibit a significant spinal deformity progression (< 15°) at skeletal maturity. Age- and sex-matched healthy control (HC) subjects were recruited from primary and high schools and were also physically examined by a seasoned spine surgeon to rule out any form of scoliosis before enrolment. All the HC subjects were interviewed about their familial antecedents, and those with a familial history of AIS, secondary or syndromic scoliosis were excluded from the study. This

study was approved by the institutional review boards of Sainte-Justine University Hospital (protocols #2018-1935), The Montreal Children's Hospital, The Shriners Hospital for Children and McGill University as well as by the Affluent and Montreal English School Boards. Written informed consents were given by parents or legal guardians and assents were obtained from all minors. All methods were carried out by relevant guidelines and human ethics regulations.

Blood specimen collection

Peripheral blood samples of participants were collected in EDTA-treated tubes and centrifuged at 216×g for 10 min. Derived plasma samples were aliquoted and stored at − 80 °C until analysis.

RNA extraction for microRNA array analysis

MiRNAs were extracted from plasma samples obtained from AIS patients and matched HC. Plasma samples were thawed and centrifugated at 17,000×g for 15 min at 4 °C. The RNA was extracted using the NucleoSpin miRNA Plasma kit (MACHEREY-NAGEL GmbH & Co. KG, Düren, Germany) according to the manufacturer's instructions.

Microarray analysis

A genome-wide expression profiling was performed for each participant in the discovery cohort at Oaklabs (Hennigsdorf, Germany), using the Agilent expression array-Human miRNA 8 × 60 K (Agilent Technologies, Santa Clara, CA, USA) harboring 2549 mature human miRNAs. We selected only miRNAs meeting the criteria: both p-value threshold is 0.05 and the $\log_2$ (Fold Change) > 0.6.

Validation of candidate miRNAs in replication cohort by qPCR

The plasma samples from the biobank cohort were thawed on ice for 15 minutes, followed by centrifugation for 15 minutes at 17,000×g at 4 °C to remove any remaining cellular debris. RNA extraction with enrichment of small RNAs was performed using the mirVana PARIS extraction kit (mirVanaPARIS RNA and Native Protein Purification Kit, Thermo Fisher Scientific, Waltham, MA, USA) according to manufacturer's instructions. 75µl of eluent solution was used to elute the RNAs from the filter cartridge, and RNA samples were stored at − 80°C. As a spike-in control, 50 nmol of Cel-miR-39-3p synthetic oligonucleotide RNA with the sequence: 5′-UCACCGGGUGUAAAUCAGCUUG-3′ (Thermo Fisher Scientific) was added to the plasma after addition of denaturing solution.

Complementary DNA (cDNA) synthesis, qPCR miRNA detection and quantification

cDNA was synthesized from the extracted miRNA samples using a PCR thermocycler (T3000 Thermocycler, Biometra, Montreal Biotech Inc., Montreal, QC, Canada) and the TaqMan Advanced miRNA cDNA Synthesis Kit (Thermo Fisher Scientific) by following manufacturer's instructions. The resulting cDNA samples were stored at − 20 °C. The synthesized cDNA was the template for qPCR using the TaqMan Advanced miRNA Assays (Thermo Fisher Scientific) and probes for each miRNA. The qPCR reaction was performed using the QuantStudio 3 instrument (Thermo Fisher Scientific). The qPCR was performed in duplicate for each sample, and the mean of the obtained cycle thresholds (CT) was used for calculations.

qPCR data analysis

The results of each miRNA for each sample were normalized with the results of the exogenous control, cel-mir-39a-3p, where ΔCTsample = CTmiR − CTcel-miR-39a-3p. Then, the ΔΔCT was calculated for each sample as follows, ΔΔCT = ΔCT sample − mean ΔCTCTRLs. Finally, the fold difference in miRNA expression between each participant and the mean of controls was calculated as $2^{(-\Delta\Delta CT)}$.

Construction of gene pathways and networks targeted by dysregulated miRNAs in AIS

The potential targets of miRNAs of interest, including genes and disease were primarily identified through the previous studies. The connections (interactions) of the miRNAs and their targets were constructed based on the Ingenuity Knowledge Base using the Ingenuity Pathway Analysis (IPA) software (QIAGEN Inc. software version 51963813).

Machine learning and statistical analyses

Random Forest Model (RFM) was applied to build the model that could predict and differentiate between Non-severe and severe groups. The data was randomly separated into training data set (80%) and testing data set (20%): the training data set was utilized to train our RFM and the testing data was used to assess the model. To evaluate our RFM, we used the different measures to achieve the performance of our predictive algorithm such as: accuracy, specificity, sensitivity, and receiver operating characteristic (ROC) curves. The ROC curves showed the trade-off between sensitivity and specificity, and the area under the curve (AUC) was used as an index for evaluating the predictive performance of the constructed miRNA panel.

Data availability

The microarray datasets generated and analyzed during the current study are available in the Gene Expression Omnibus (GEO) repository, accession number GSE286204. Other datasets are available from the corresponding author on reasonable request.

Received: 4 November 2024; Accepted: 3 February 2025

Published online: 12 February 2025

References

1. Cheng, J. C. et al. Adolescent idiopathic scoliosis. *Nat. Rev. Dis. Primers*. **1**, 15030 (2015).
2. Liu, H. et al. miR-21 promotes human nucleus pulposus cell proliferation through PTEN/AKT signaling. *Int. J. Mol. Sci.* **15**, 4007–4018 (2014).
3. Zheng, J., Yang, Y., Zhao, K. & Wang, R. Low expression of microRNA-143 is related to degenerative scoliosis possibly by regulation of cyclooxygenase-2 expression. *Int. J. Clin. Exp. Med.* **8**, 4140 (2015).
4. Yeh, C. H., Jin, L., Shen, F., Balian, G. & Li, X. J. miR-221 attenuates the osteogenic differentiation of human annulus fibrosus cells. *Spine J.* **16**, 896–904 (2016).
5. Ogura, Y. et al. A functional variant in MIR4300HG, the host gene of microRNA MIR4300 is associated with progression of adolescent idiopathic scoliosis. *Hum. Mol. Genet.* **26**, 4086–4092 (2017).
6. Zhang, J. et al. Aberrant miR-145-5p/beta-catenin signal impairs osteocyte function in adolescent idiopathic scoliosis. *FASEB J.* fj201800281 (2018).
7. García-Giménez, J. L. et al. Circulating miRNAs as diagnostic biomarkers for adolescent idiopathic scoliosis. *Sci. Rep.* **8**, 2646 (2018).
8. Hui, S. et al. Differential miRNAs profile and bioinformatics analyses in bone marrow mesenchymal stem cells from adolescent idiopathic scoliosis patients. *Spine J.* **19**, 1584–1596 (2019).
9. Li, J. et al. Suv39h1 promotes facet joint chondrocyte proliferation by targeting miR-15a/Bcl2 in idiopathic scoliosis patients. *Clin. Epigenet.*. **11**, 107 (2019).
10. Huang, F. et al. Incidence of scoliosis among junior high school students in Zhongshan city, Guangdong and the possible importance of decreased miR-30e expression. *J. Int. Med. Res.* **48**, 0300060519889438 (2020).
11. Wang, Y. et al. Dysregulated bone metabolism is related to high expression of miR-151a-3p in severe adolescent idiopathic scoliosis. *Biomed. Res. Int.* **2020** (2020).
12. Hou, C., Li, B., Cheng, Y., Li, M. & Yang, Z.D. Upregulation of cGMP-dependent protein kinase (PRKG1) in the development of adolescent idiopathic scoliosis. *Orthop. Surg.* **12**, 1261–1269 (2020).
13. Chen, W. K. et al. LncRNA HOTAIR influences cell proliferation via miR-130b/PTEN/AKT axis in IDD. *Cell. Cycle*. **21**, 323–339 (2022).
14. Chen, H. et al. Upregulation of microRNA-96-5p is associated with adolescent idiopathic scoliosis and low bone mass phenotype. *Sci. Rep.* **12**, 9705 (2022).
15. Raimondi, L. et al. Investigating the Differential circulating microRNA expression in adolescent females with severe idiopathic scoliosis: a proof-of-concept observational clinical study. *Int. J. Mol. Sci.* **25**, 570 (2024).
16. Horak, M., Novak, J. & Bienertova-Vasku, J. J. D. .b. muscle-specific microRNAs in skeletal muscle development. **410**, 1–13 (2016).
17. Li, H. M. et al. In silico analysis excavates a novel competing endogenous RNA subnetwork in adolescent idiopathic scoliosis. *Front. Med.* **7**, 583243 (2020).
18. Dinesh, N. E., Campeau, P. M. & Reinhardt, D. P. Fibronectin isoforms in skeletal development and associated disorders. **323**, C536–C549 (2022).
19. Falls, C. J., Page, P. S., Stadler, J. A. & StadlerIII J.A.J.C. Operative management of spinal deformity secondary to Hajdu-Cheney syndrome. **13** (2021).
20. Dai, Z. et al. Novel mutations in UTS2R are associated with adolescent idiopathic scoliosis in the Chinese population. **46**, E288–E293 (2021).
21. Zhang, X. et al., Cilia-driven cerebrospinal fluid flow directs expression of urotensin neuropeptides to straighten the vertebrate body axis. **50**, 1666–1673 (2018).
22. Amor, I. B. et al., Severe osteogenesis imperfecta caused by a small in-frame deletion in CRTAP. **155**, 2865–2870 (2011).
23. Fendri, K. et al. Microarray expression profiling identifies genes with altered expression in adolescent idiopathic scoliosis. **22**, 1300–1311 (2013).
24. Shi, B. et al. Abnormal PITX1 gene methylation in adolescent idiopathic scoliosis: a pilot study. *BMC Musculoskelet. Disord.* **19**, 1–6 (2018).
25. Jin, B., Li, Y. & Robertson, K. D. DNA methylation: superior or subordinate in the epigenetic hierarchy? *Genes cancer*. **2**, 607–617 (2011).
26. Chan, M. H., Merrill, S. M., Konwar, C. & Kobor, M. S. An integrative framework and recommendations for the study of DNA methylation in the context of race and ethnicity. *Discover Social Sci. Health*. **3**, 9 (2023).
27. Gao, W. et al., Rare coding variants in MAPK7 predispose to adolescent idiopathic scoliosis. **38**, 1500–1510 (2017).
28. Zhou, T. et al., Mutant MAPK7-induced idiopathic scoliosis is linked to impaired osteogenesis. **48**, 880–890 (2018).
29. Bredoux, R. et al., Human platelet Ca2+-ATPases: new markers of cell differentiation as illustrated in idiopathic scoliosis. **17**, 421–433 (2006).
30. Gao, X. et al., CHD7 gene polymorphisms are associated with susceptibility to idiopathic scoliosis. **80**, 957–965 (2007).
31. Wang, W. et al. Predictive value of single-nucleotide polymorphisms in curve progression of adolescent idiopathic scoliosis. **31**, 2311–2325 (2022).
32. Nada, D. et al., Association of circulating YKL-40 levels and CHI3L1 variants with the risk of spinal deformity progression in adolescent idiopathic scoliosis. **9**, 5712 (2019).
33. Shidfar, A. et al., Expression of miR-18a and miR-210 in normal breast tissue as candidate biomarkers of breast cancer risk. **10**, 89–97 (2017).
34. Favier, A. et al., MicroRNA as epigenetic modifiers in endometrial cancer: a systematic review. **13**, 1137 (2021).
35. Xu, P. et al., miR-18a contributes to preeclampsia by downregulating Smad2 (full length) and reducing TGF-β signaling. **22**, 542–556 (2020).
36. Castellano, L. et al. The estrogen receptor-α-induced microRNA signature regulates itself and its transcriptional response. *Proc. Natl. Acad. Sci.* **106**, 15732–15737 (2009).

Acknowledgements

We thank the patients and families who participated in this study, and the orthopedic surgeons and nursing teams at Sainte-Justine University Hospital (CHU Sainte-Justine), The Children's Hospital and The Shriners Hospital. This work was supported by grants to Dr. Alain Moreau from MEDTEQ (Ministère du Dévelopement Économique et de l'Innovation du Québec), Medtronic Canada, La Fondation Yves Cotrel de l'Institut de France (Paris, France) and The Montreal TransMedTech Institute. Similarly, Ms. Nasrin Khatami and Dr. Iurie Caraus were supported by a doctoral and postdoctoral scholarship respectively from MITACS (Canada).

Author contributions

N.K., A.F., M. B., A.-M. L., S.P., H.L., C-É. A., J.L., and A.M. designed the research project; N.K., E.N., and I.C. performed the analyses; I.C. contributed to the development of new analytic tools; N.K., I.C., and A.M. analyzed data; N.K., W.E and A.M. wrote the initial version of the manuscript; N.K., E.N., M.R., M.E., W.E., and A.F helped run experiments; and N.K performed IPA analysis. All co-authors reviewed and approved the manuscript.

Declarations

Competing interests

This work led to a patent application (pending) own by CHU Sainte-Justine. All other authors declare no other potential conflicts of interest.

Additional information

Supplementary Information The online version contains supplementary material available at https://doi.org/10.1038/s41598-025-88985-3.

Correspondence and requests for materials should be addressed to A.M.

Reprints and permissions information is available at www.nature.com/reprints.

Publisher's note Springer Nature remains neutral with regard to jurisdictional claims in published maps and institutional affiliations.

Open Access This article is licensed under a Creative Commons Attribution-NonCommercial-NoDerivatives 4.0 International License, which permits any non-commercial use, sharing, distribution and reproduction in any medium or format, as long as you give appropriate credit to the original author(s) and the source, provide a link to the Creative Commons licence, and indicate if you modified the licensed material. You do not have permission under this licence to share adapted material derived from this article or parts of it. The images or other third party material in this article are included in the article's Creative Commons licence, unless indicated otherwise in a credit line to the material. If material is not included in the article's Creative Commons licence and your intended use is not permitted by statutory regulation or exceeds the permitted use, you will need to obtain permission directly from the copyright holder. To view a copy of this licence, visit http://creativecommons.org/licenses/by-nc-nd/4.0/.

© The Author(s) 2025